

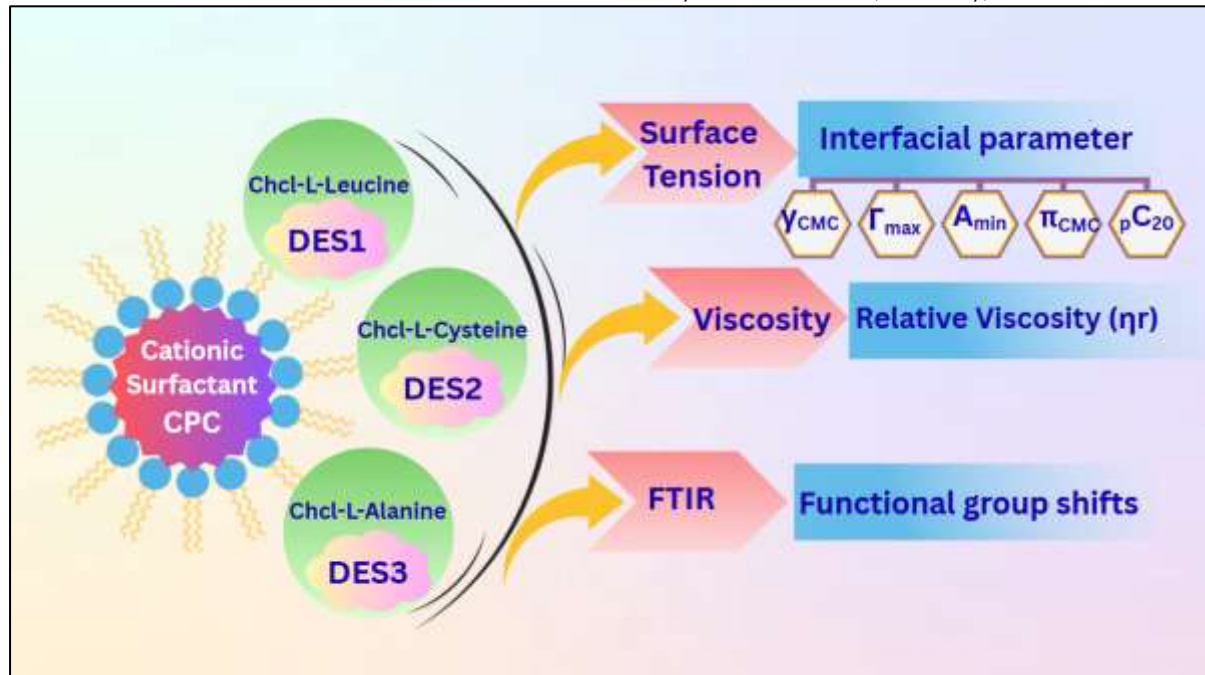
Interfacial And Structural Insights Into Cetylpyridinium Chloride-Deep Eutectic Solvent Systems: A Surface Tension, Viscosity And FTIR Study

Namrata Tamboli^a and Prashant Mundeja^b

^{a,b}School of Sciences, MATS University, Raipur, Chhattisgarh, India

Graphical Abstract-

Interaction of amino acid-based DESs with CPC studied by surface tension, viscosity, and FTIR Method



Abstract

This study investigates the interfacial and structural behavior of cetylpyridinium chloride (CPC) in the presence of three amino acid-based deep eutectic solvents (DESs) synthesized from choline chloride with L-leucine (DES1), L-cysteine (DES2), and L-alanine (DES3). Surface tension analysis revealed that the addition of DESs significantly reduced the critical micelle concentration (CMC) of CPC, accompanied by variations in interfacial parameters such as surface tension at CMC (γ_{CMC}), surface pressure at CMC (π_{CMC}), maximum surface excess concentration (Γ_{max}), minimum surface area per molecule (A_{min}), and adsorption efficiency (pC_{20}). Among the systems, DES1 at 1.0 wt% exhibited the strongest reduction in CMC and enhanced π_{CMC} , attributed to hydrophobic interactions from leucine side chains. DES2 displayed higher Γ_{max} and pC_{20} values, indicating efficient adsorption and compact interfacial packing through thiol-mediated interactions, whereas DES3 exerted comparatively weaker effects. Viscosity measurements confirmed micellar growth, with DES2 promoting elongated or worm-like aggregates that enhanced flow resistance. FTIR spectroscopy further supported these findings, showing hydrogen bonding, electrostatic interactions, and shifts in vibrational bands that validate structural modifications. Overall, the results demonstrate that amino acid-based DESs can effectively modulate CPC micellization, offering promising insights into surfactant-DES interactions for sustainable formulations and green chemistry applications.

Keywords Deep eutectic solvents, CPC, Surface tension, Viscosity, FTIR

1. INTRODUCTION-

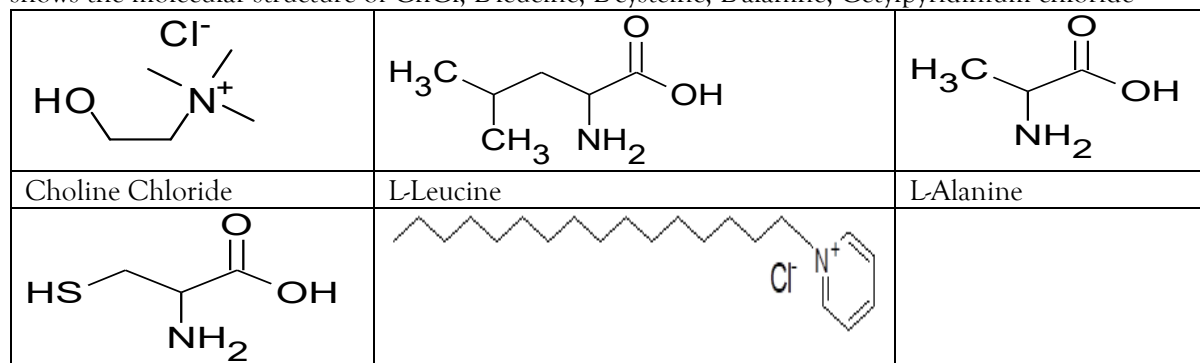
Deep eutectic solvents (DESs) represent an emerging class of environmentally friendly solvents, characterized by their facile preparation from a combination of hydrogen bond acceptors (HBAs) and hydrogen bond donors (HBDs) [1-2]. Their defining attribute is the significant depression of melting points due to strong intermolecular hydrogen bonding, which provides DESs with unique physicochemical properties advantageous for green chemistry applications [3-5]. Owing to their biodegradability, low toxicity, low volatility, and cost-effectiveness, DESs have garnered increased attention as sustainable alternatives to conventional organic solvents in fields such as extraction, catalysis, electrochemistry, and

drug delivery [6–8]. Among these, amino acid-based DESs have attracted particular interest because amino acids are naturally derived, biodegradable, and possess diverse side chains offering versatile chemical functionalities [9-11]. The side chains, ranging from hydrophobic alkyl groups to functional groups such as thiols, play a critical role in modulating the properties of the resultant DESs, impacting solvent behavior and interaction capabilities with solutes [12–13]. Surfactants, molecules comprising hydrophilic and hydrophobic moieties, have an inherent ability to self-assemble in solution, forming micelles beyond a critical micelle concentration (CMC) that significantly influences interfacial phenomena [14-15]. Cetylpyridinium chloride (CPC), a cationic surfactant bearing a long hydrophobic alkyl chain and a positively charged pyridinium headgroup, is widely used due to its potent surface activity and antimicrobial properties [16-18]. The interfacial and aggregate behavior of CPC is crucial in applications spanning pharmaceuticals, cosmetics, and material synthesis. The interplay between surfactants and DESs is of growing interest, as DESs can profoundly affect the aggregation behavior and interfacial properties of surfactants through hydrogen bonding, electrostatic, and hydrophobic interactions [19-20]. Thus, studying CPC in the presence of amino acid-based DESs provides insights into the modulation of surfactant properties in sustainable solvent media. This study aims to systematically explore the effect of three amino acid-based DESs ChCl-L-leucine (DES1), ChCl-L-cysteine (DES2), and ChCl-L-alanine (DES3) on the micellization and interfacial behavior of CPC. Utilizing surface tension measurements to determine CMC and interfacial parameters, viscosity to probe bulk solution properties, and Fourier-transform infrared (FTIR) spectroscopy to investigate molecular interactions, this work elucidates the role of amino acid composition in tuning surfactant aggregation and adsorption. The findings contribute fundamental knowledge guiding the design of green solvent-surfactant systems for pharmaceutical and chemical applications.

2. MATERIALS AND METHODS

2.1 Materials

Three amino acids (L-leucine (purity $\geq 99\%$), L-cysteine (purity $\geq 99\%$), and L-alanine (purity $\geq 99\%$)), Choline Chloride (ChCl with purity $\geq 99\%$), Methyl Orange (purity $\geq 99\%$) and Cetylpyridinium chloride (CPC with purity $\geq 99\%$) were purchased from Sigma Aldrich Pvt. Ltd and used for the synthesis of DESs without further purification. All the aqueous solutions were prepared with Millipore water. Figure 1 shows the molecular structure of ChCl, L-leucine, L-cysteine, L-alanine, Cetylpyridinium chloride



L-Cysteine Cetylpyridinium chloride

Fig-1: Molecular Structure of ChCl, L-leucine, L-cysteine, L-alanine and Cetylpyridinium chloride

2.2 Methods

2.2.1 Surface Tension Measurement

Surface tension of the solutions was measured with a stalagmometer (ABGIL Borosilicate, India), which was calibrated using double-distilled water. The drop count method was applied, where the number of drops formed from a fixed volume of solution passing through a capillary was recorded. For each solution, measurements were repeated twice to ensure reproducibility. Using the drop numbers obtained for pure water and test solutions, surface tension values were calculated, and the corresponding critical micelle concentration (CMC) was determined. The experimental data were plotted to highlight the variations and comparative behavior of the systems.

2.2.2 Viscosity Measurement

Viscosity studies were performed using an Ostwald viscometer. The viscometer was filled with the prepared solutions up to the marked level, and liquid flow between two calibration points was timed with a digital stopwatch (accuracy ± 0.01 s) at 299 K. Measurements were carried out at different concentrations

(0.5% and 1.0% by weight). The relative viscosity of each solution was calculated by taking the ratio of solution viscosity to solvent viscosity. All experiments were conducted in duplicate, and the mean values were considered for further analysis. The results were graphically represented to show concentration-dependent trends.

2.2.3 Fourier Transform Infrared (FTIR) Spectroscopy

FTIR spectra were obtained using a Bruker Optics spectrophotometer (Germany) through the KBr pellet method. Samples were prepared by mixing 1 mg of the compound with 100 mg of KBr and pressing them into transparent disks. Spectral measurements were recorded in the range of 4000–400 cm^{-1} at room temperature. FTIR analysis was performed for all synthesized DESs (DES1: ChCl:L-leucine, DES2: ChCl:L-cysteine, DES3: ChCl:L-alanine), along with pure choline chloride, CPC surfactant. The spectra were used to identify functional groups and possible molecular interactions among the components.

2.2.4. Preparation of DESs

The deep eutectic solvents (DESs) were prepared by mixing choline chloride, acting as the hydrogen bond acceptor (HBA), with the amino acids L-leucine, L-cysteine, or L-alanine, which served as hydrogen bond donors (HBDs). A fixed molar ratio of 1:2 (HBA:HBD) was maintained for all preparations. The mixtures were heated at 80–100 °C under constant stirring until a clear and homogeneous liquid was formed. The obtained DESs were then cooled to room temperature, transferred into amber glass vials, and sealed tightly to avoid moisture uptake. No further purification was necessary.

3. RESULTS AND DISCUSSION

3.1. Surface tension study

Surface tension measurements provide valuable insight into the micellization process and interfacial adsorption of surfactants, in the presence of deep eutectic solvents (DESs). In the present work, cetylpyridinium chloride (CPC), a cationic surfactant, was selected to evaluate its self-assembly behavior in aqueous medium and in the presence of three amino acid-based DESs: ChCl:L-leucine (DES1), ChCl:L-cysteine (DES2), and ChCl:L-alanine (DES3). The primary objective of this study was to determine the critical micelle concentration (CMC) and related interfacial parameters, thereby understanding how amino acid-based DESs influence the aggregation and adsorption efficiency of CPC at the air-water interface.

As expected, the surface tension of CPC solutions decreased progressively with increasing surfactant concentration, followed by a distinct breakpoint corresponding to micelle formation. This transition point, defined as the CMC, was carefully evaluated in the absence and presence of DESs to assess their modulatory effects on micellization. Figure 2 illustrates the surface tension concentration plots for CPC alone and in combination with 0.5 and 1.0 wt% of each DES. The curves clearly demonstrate that all three DESs alter the slope of the pre-micellar region and shift the CMC, indicating their direct involvement in modifying surfactant packing and interfacial adsorption. The CMC values of CPC, obtained by the surface tension method, in the presence of 0.5 and 1.0 wt% of ChCl:L-leucine (DES1), ChCl:L-cysteine (DES2), and ChCl:L-alanine (DES3) are summarized in Table 1.

At 0.5 wt% DES concentration, minor but significant differences were observed among the three systems. For DES1 (ChCl:L-leucine), a moderate decrease in CMC was detected, suggesting that the hydrophobic isobutyl group of leucine enhanced the tendency of CPC molecules to self-assemble. DES2 (ChCl:L-cysteine) also reduced surface tension, but the effect was relatively weaker, likely due to specific interactions of the -SH group with CPC headgroups that hindered close packing at the air-water interface. In contrast, DES3 (ChCl:L-alanine) showed minimal effect, with only a slight lowering of surface tension, indicating poor efficiency in modifying CPC micellization at low concentrations.

At 1.0 wt% DES concentration, the modulation became more pronounced. DES1 exhibited the strongest reduction in CMC and enhanced surface pressure at CMC (πCMC), confirming that leucine units significantly stabilize micellar aggregates through hydrophobic interactions and efficient interfacial adsorption. DES2 also displayed a notable decrease in surface tension at this concentration, reflecting stronger hydrogen bonding and electrostatic interactions, although less effective than leucine-based DES. DES3 again showed the weakest impact, suggesting that the small methyl group of alanine lacks the capacity to drive CPC aggregation effectively. Overall, the sequence of DES influence on CPC micellization followed the trend:

DES1 (ChCl:L-leucine) > DES2 (ChCl:L-cysteine) > DES3 (ChCl:L-alanine)

Banjare et al., Investigating cationic surfactants in glycerol-based DES (Glyceline) and water mixtures, the authors used tensiometry to derive CMC, surface excess (Γ), and other interfacial parameters. Results

indicated that increasing DES content lowers the CMC and promotes aggregation compared to pure water, attributed to enhanced interactions between DES components and surfactant headgroups [21]. Johnson et al., investigated sodium dodecyl sulfate (SDS) in glycine and reline DESs, employing surface-tension analysis to monitor micellization. The study reported sharper breakpoints and distinct pre-CMC slopes compared with water, indicating modified interfacial adsorption. Complementary microscopy confirmed the formation of dendritic aggregates, suggesting unique self-assembly processes in DES media [22].

Table 1. The critical micelle concentration (CMC) of CPC, determined from surface tension measurements, was evaluated in the presence of 0.5 and 1.0 wt% of three biologically active amino acid-based deep eutectic solvents: ChCl:L-leucine (DES1), ChCl:L-cysteine (DES2), and ChCl:L-alanine (DES3).

Concentration of DES (wt%)	CMC (M)		
	ChCl-L-Leucine(DES1)	ChCl-L-Cysteine(DES2)	ChCl-L-Alanine (DES3)
0.5	0.000566± 0.0000020	0.000825± 0.0000030	0.00074± 0.0000020
1.0	0.000476± 0.0000020	0.00074± 0.0000020	0.000654± 0.0000020

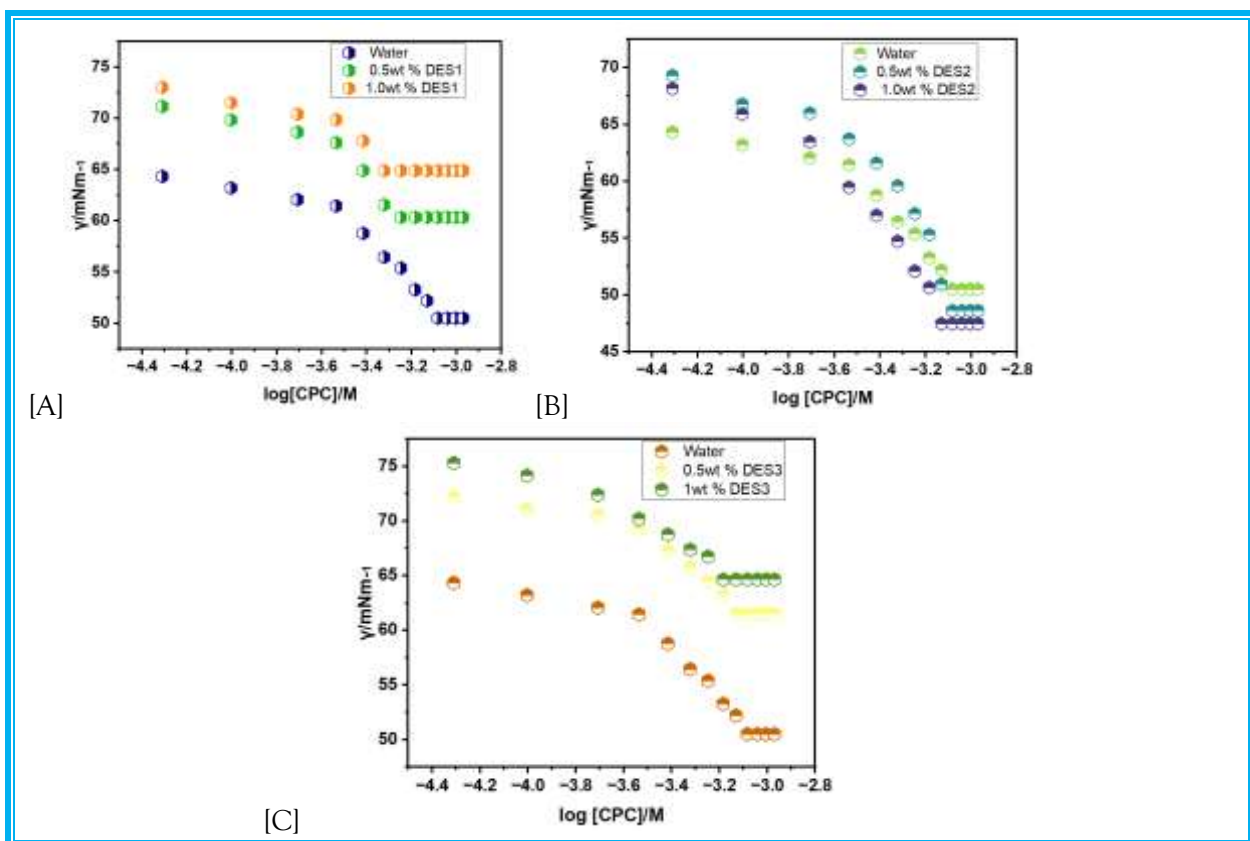


Fig-2. Plotted surface tension against (log[CPC]/M) within 0.5wt% and 1.0wt% of [A] DES1 + CPC, [B] DES2 + CPC, and [C] DES3 + CPC

3.2 Comparative Interfacial Analysis of CPC in L-Leucine, L-Cysteine, and L-Alanine Based DESs-

In the present investigation, Eqs. (1)-(5) were applied to evaluate the interfacial parameters of CPC and to examine the influence of DESs on properties such as the surface tension at CMC (γ_{CMC}), the surface pressure at CMC (π_{CMC}), the efficiency of adsorption (pC_{20}), the minimum surface area per molecule (A_{min}), and the maximum surface excess concentration (Γ_{max}). The surface activity of CPC was systematically determined in aqueous medium containing 0.5 and 1.0 wt% of three biologically active DESs, namely ChCl:L-leucine (DES1), ChCl:L-cysteine (DES2), and ChCl:L-alanine (DES3).

3.2.1 The maximum surface excess concentration (Γ_{max})

$$\Gamma_{max} = \left(\frac{1}{2.303nRT} \right) \left(\frac{d\gamma}{d \log_{10} C} \right) T p [1] \quad (1)$$

Where $\left(\frac{d\gamma}{d \log_{10} C}\right)$ yields the slope of the surface tension isotherm close to the critical mass, R is the gas constant (8.314 J mol⁻¹ K⁻¹), and C is the concentration of the CPC. Pre-factor (n = constant) value has been taken for 2, γ_{CMC} is the surface tension at CMC, γ_0 is the surface tension of pure water, absolute temperature (T) in Kelvin, and N_A is Avogadro's number. At 299 K, the surface excess concentration Γ_{max} of cationic surfactant CPC was found to decrease upon the incorporation of 0.5 and 1.0 wt% deep eutectic solvents (DESs) formulated with amino acids such as L-leucine (DES1), L-cysteine (DES2), and L-alanine (DES3). This reduction is attributed to the enhanced surface activity of the DESs, which promotes greater accumulation of CPC molecules at the air-water interface. Among the systems examined, the trend in Γ_{max} values followed the order: DES2 > DES3 > DES1. Particularly, the L-cysteine-based DES at 1.0 wt% exhibited more efficient adsorption at the air/solution interface, likely due to a decrease in electrostatic repulsion among the cationic head groups of CPC.

3.2.2 The surface pressure at the CMC (π_{CMC})

$$\pi_{CMC} = \gamma_0 - \gamma_{CMC} \quad (2)$$

Where π_{CMC} denotes the solutions' surface tension at CMC and γ_0 denotes the surface tension of distilled water. γ_{CMC} is the surface tension at CMC. The π_{CMC} of CPC is subjected to different interactions that facilitate the effective adsorption of 0.5 and 1.0 wt% of DESs such as L-leucine (DES1), L-cysteine (DES2) and L-alanine (DES3) at the air-water interface of the solutions. The maximum values of π_{CMC} have indicated more effective adsorption at the CPC interface due to the polar-non-polar repulsion of the 1wt% DES1 system being significantly higher than the DES2 and DES3 system repulsions. The resulting order of π_{CMC} is DES2 > DES1 > DES3.

3.2.3 The minimum area per molecule (A_{min})

The adsorbed surfactant molecule's degree of packing and orientation is revealed by the minimum surface area per molecule (A_{min}). Applying the Gibbs adsorption isotherm, the minimum area per molecule (A_{min}) occupied by a single amphiphilic molecule at the air-water interface was computed.

$$A_{min} = \left(\frac{1}{\Gamma_{max}}\right) N_A \quad [3]$$

The minimum area per molecule is inversely proportional to the maximum surface excess concentration, so the higher Γ_{max} value lowers the comparison to the A_{min} value. The order found for A_{min} is: DES3 > DES1 > DES2. This indicates that the molecules are less tightly packed for flexibility at the air-water contact. The A_{min} values increase with an increase in the 0.5 and 1 wt% of DESs for cationic CPC. It could be demonstrated that the effect of DESs reduced the surface area of the CPC molecule accessible.

3.2.4. The efficiency of adsorption (pC_{20})

The following equation (4) is used to determine the adsorption efficiency (pC_{20}):

$$pC_{20} = -\log_{10} C_{20} \quad [4]$$

The calculated pC_{20} values of the CPC system have increased as the wt% of DESs has increased. The efficiency of adsorption on CPC forms micelles reduces the number of micellar solution interfaces in the system. The concentration of the cationic CTAB surfactant, which lowers the surface tension of the pure solvent by 20 mN/m, is represented by the negative log, pC_{20} , in this equation. The efficiency of amphiphilic molecules for adsorption at the air/water interface is normally determined by the bulk concentration of these molecules, which causes a surface tension reduction observed at 20 mNm⁻¹ (pC_{20}) from the pure solvent. Their negative logarithm of C_{20} ($-\log C_{20}$) is called pC_{20} , and a higher value indicates a larger adsorption efficiency. Due to its higher hydrophobicity, pure CPC has a higher pC_{20} value except for a mixture of DESs, which was seen in Table 2. Higher pC_{20} values have shown that the combinations of CPC and DESs are more surface active than their solo components. The order found for pC_{20} is: DES2 > DES3 > DES1.

Concentration of DES (wt%)	γ_{CMC} (mNm ⁻¹)	Γ_{max} (mol ⁻²)10 ⁶	A_{min} (m ² mol ⁻¹)10 ²⁰	π_{CMC} (mNm ⁻¹)	pC_{20}
Water	32.0±0.10	2.17±0.11	0.721±0.010	34.0±6.35	3.76±0.03
ChCl-L-Leucine (DES1)					
0.5	60.34± 0.13	1.79±0.09	0.0927±0.0035	11.6±1.08	2.68 ±0.04

1.0	64.89±0.12	1.60±0.12	0.1038±0.0032	7.11±1.08	2.509 ±0.03
ChCl-L-Cysteine (DES2)					
0.5	48.63± 0.10	3.07±0.10	0.0543±0.0028	23.37±1.08	3.17±0.07
1.0	47.48±0.11	3.16±0.08	0.0526±0.0030	24.52±1.04	3.24 ±0.07
ChCl-L-Alanine (DES3)					
0.5	61.51±0.14	1.53±0.07	0.1086±0.0041	10.49±0.93	2.52 ±0.08
1.0	64.65±0.12	1.58±0.06	0.1052±0.0038	7.35±0.93	3.93 ±0.04

3.3. Viscosity study of CPC within amino acid-based DESs

The variation of relative viscosity (η_r) with increasing concentration of CPC in the absence and presence of DES1, DES2, and DES3 is presented in Figures 3 [A]-[C]. In all systems, η_r increases progressively with surfactant concentration and reaches a plateau after the critical micelle concentration (CMC), suggesting micelle formation and subsequent stabilization. However, the magnitude and trend of viscosity changes depend strongly on the type and concentration of the deep eutectic solvents (DESs).

For DES1 (ChCl + L-leucine), both 0.5 wt% and 1.0 wt% systems show enhanced viscosity compared to water. At lower CPC concentrations, 1.0 wt% DES1 exhibits the highest η_r values, indicating stronger interaction between CPC and DES1. This may be attributed to hydrogen bonding and electrostatic interactions of the amino acid moiety with CPC headgroups, promoting micelle growth. After the CMC, viscosity values for 1.0 wt% DES1 plateau slightly below water, suggesting steric hindrance may restrict micellar packing at higher surfactant concentrations.

In the case of DES2 (ChCl + L-cysteine), a distinctly different trend is observed. At lower concentrations, η_r in 0.5 wt% DES2 is slightly below that in water, whereas 1.0 wt% DES2 shows a remarkable increase. The sharp rise in viscosity with 1.0 wt% DES2 indicates strong micelle-DES interactions, possibly due to the thiol group of cysteine providing additional binding sites with CPC. The higher η_r values beyond the CMC suggest formation of elongated or worm-like micelles stabilized by DES2, resulting in increased resistance to flow.

For DES3 (ChCl + L-alanine), the trend shows a moderate effect compared to DES1 and DES2. At lower CPC concentrations, η_r values with 0.5 wt% DES3 are slightly suppressed, while 1.0 wt% DES3 shows values comparable to water. However, beyond the CMC, both DES3 systems exhibit higher viscosity compared to CPC in water, with 0.5 wt% DES3 showing the strongest enhancement. This indicates that alanine-based DES promotes micelle growth and packing density, possibly through hydrophobic association with the surfactant tail region. Overall, the viscosity data clearly demonstrate that the incorporation of DESs alters the micellization behavior of CPC. Among the three systems, DES2 shows the strongest synergistic effect with CPC, leading to significantly enhanced viscosity and suggesting the formation of more structured micellar aggregates. DES1 and DES3 also influence micellization but with comparatively weaker effects, highlighting the role of amino acid functional groups in tuning surfactant-DES interactions.

Manasi, King, and Edler (2024) focused on cationic micelles across different DES compositions and explicitly related micelle formation and morphology to bulk transport properties, including viscosity. They showed that small compositional changes (HBA/HBD identity and ratio, plus water content) change the effective viscosity experienced by surfactants and therefore the equilibrium and kinetics of micellization. The paper reinforces a recurring practical point: when reporting viscosity-related surfactant data in DESs, authors must state DES mole ratios, water content and temperature because small changes produce large viscosity shifts that strongly affect micelle behaviour [23]. Gajardo-Parra et al., provided a careful experimental and modeling study of the viscosity of many ChCl-based DESs and their temperature dependence; while not a surfactant study per se, this work is frequently used as the viscosity reference for subsequent DES-surfactant papers. Their dataset and fitted models make it easy to distinguish intrinsic DES viscosity effects from those caused by added surfactant or additives: for example, authors can compare measured viscosities after surfactant addition to the predicted baseline viscosity (at the same temperature and composition) to quantify surfactant-induced structuring or dilution effects. For DES-surfactant work this gives a rigorous baseline for discussing viscosity changes upon micellization [24].

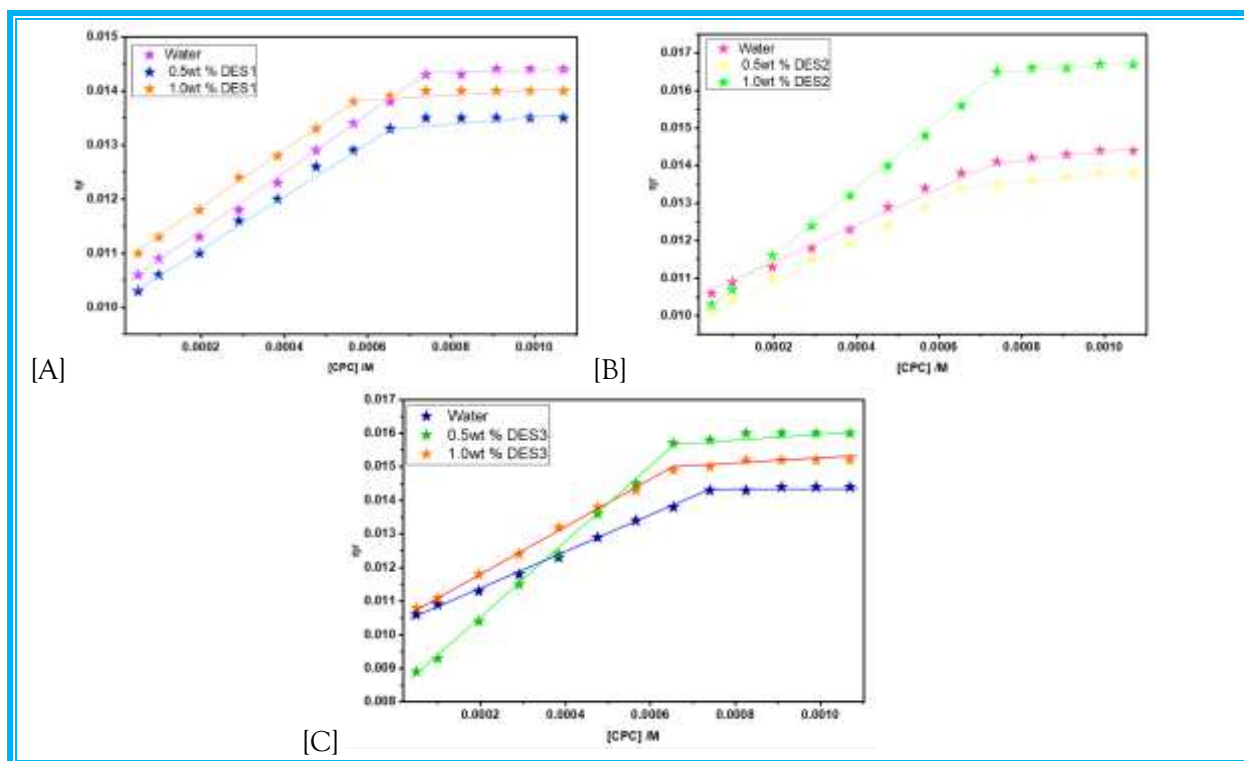


Fig 3 [A]-[C] Plotted relative viscosities against ($\log[\text{CPC}]/\text{M}$) within 0.5wt% and 1.0wt% of DESs with CPC

3.4 FTIR study

Fourier Transform Infrared (FTIR) spectroscopy is a powerful analytical technique widely employed to elucidate the molecular interactions and structural features of complex chemical systems. In this work, FTIR analysis was conducted on mixtures of cetylpyridinium chloride (CPC) with three different deep eutectic solvents (DES1, DES2, and DES3) to understand the nature of hydrogen bonding, functional group changes, and molecular associations. FTIR provides detailed insight into the vibrational modes of chemical bonds such as O-H, N-H, C-H, C=O, C-N, and C-O, which are indicative of specific functional groups and their interaction environments show in Table 3. By systematically examining the FTIR spectra of CPC combined with each DES, we gain crucial information about how the DES composition influences CPC's molecular environment. This evaluation is vital for optimizing the physicochemical properties and developing advanced materials or formulations based on these DES-CPC systems. The following sections describe the prominent absorption bands observed for each combination, highlighting shifts in peak positions and intensities that reveal changes in hydrogen bonding, dipole interactions, and molecular conformations.

The FTIR spectrum for DES1 + CPC Figure 4 [A] reveals a broad O-H stretching band at 3374.67 cm^{-1} , indicative of strong hydrogen bonding interactions within the matrix. N-H stretching is observed at 3188.10 cm^{-1} , confirming the presence of amine groups. Multiple C-H stretching peaks (3053.19 , 3006.89 , 2955.55 , and 2913.02 cm^{-1}) are characteristic of both aromatic and aliphatic chains from CPC and the DES. The C=O stretching vibration at 1668.38 cm^{-1} suggests carbonyl-containing DES components, while the C-N stretching at 1091.06 cm^{-1} reflects heteroatom-linked functionalities. The C-O stretching bands appear at 1237.44 and 1262.43 cm^{-1} . CH_2/CH_3 bending vibrations are present at 1462.50 and 1414.36 cm^{-1} , with an out-of-plane C-H bending mode at 886.38 cm^{-1} .

For DES2 + CPC Figure 4 [B] the O-H stretching band is found at 3375.82 cm^{-1} , suggesting similar hydrogen bonding networks as DES1. No prominent N-H stretching is observed. C-H stretching vibrations (3048.90 , 3006.10 , 2911.61 , and 2848.45 cm^{-1}) reflect the hydrocarbon structure. The C=O stretching occurs at 1629.35 cm^{-1} , and C-N stretching is evident at 1085.46 and 1049.88 cm^{-1} . C-O stretching peaks are at 1299.88 and 1205.29 cm^{-1} . Bending vibrations (CH_2/CH_3) are observed at 1478.45 and 1405.15 cm^{-1} , and out-of-plane C-H bending appears at 875.39 and 845.02 cm^{-1} .

In DES3 + CPC Figure 4 [C] O-H stretching bands are prominent at both 3545.55 and 3374.25 cm^{-1} , with N-H stretching at 3191.64 cm^{-1} . The C-H stretching appears at 3048.17 , 3006.44 , 2952.24 , and 2911.95 cm^{-1} , indicating multiple hydrocarbon environments. C=O stretching is split, observed at

1666.28 and 1638.40 cm^{-1} , while C-N stretching is at 1066.66 and 1012.60 cm^{-1} . C-O stretches are present at 1235.57 and 1209.38 cm^{-1} . Bending (CH_2/CH_3) vibrations at 1471.15 and 1409.32 cm^{-1} and out-of-plane C-H bands at 847.59 and 818.24 cm^{-1} are also recorded.

Sarkar et al., used FTIR to analyze the self-assembly of short-chain ionic liquid surfactants in ChCl-based DESs. FTIR band shifts in CH_2 stretching vibrations and headgroup regions supported changes in surfactant packing and strong interactions with the DES hydrogen-bond donor, providing direct spectroscopic evidence for modified micellization behavior in DESs [25]. Singh et al., demonstrated through FTIR that amino acid-based DESs interact strongly with SDS micelles. The shifts in amide and hydroxyl stretching vibrations confirmed that amino acid functional groups directly interact with surfactant headgroups, thereby influencing micellar size and aggregation number [26].

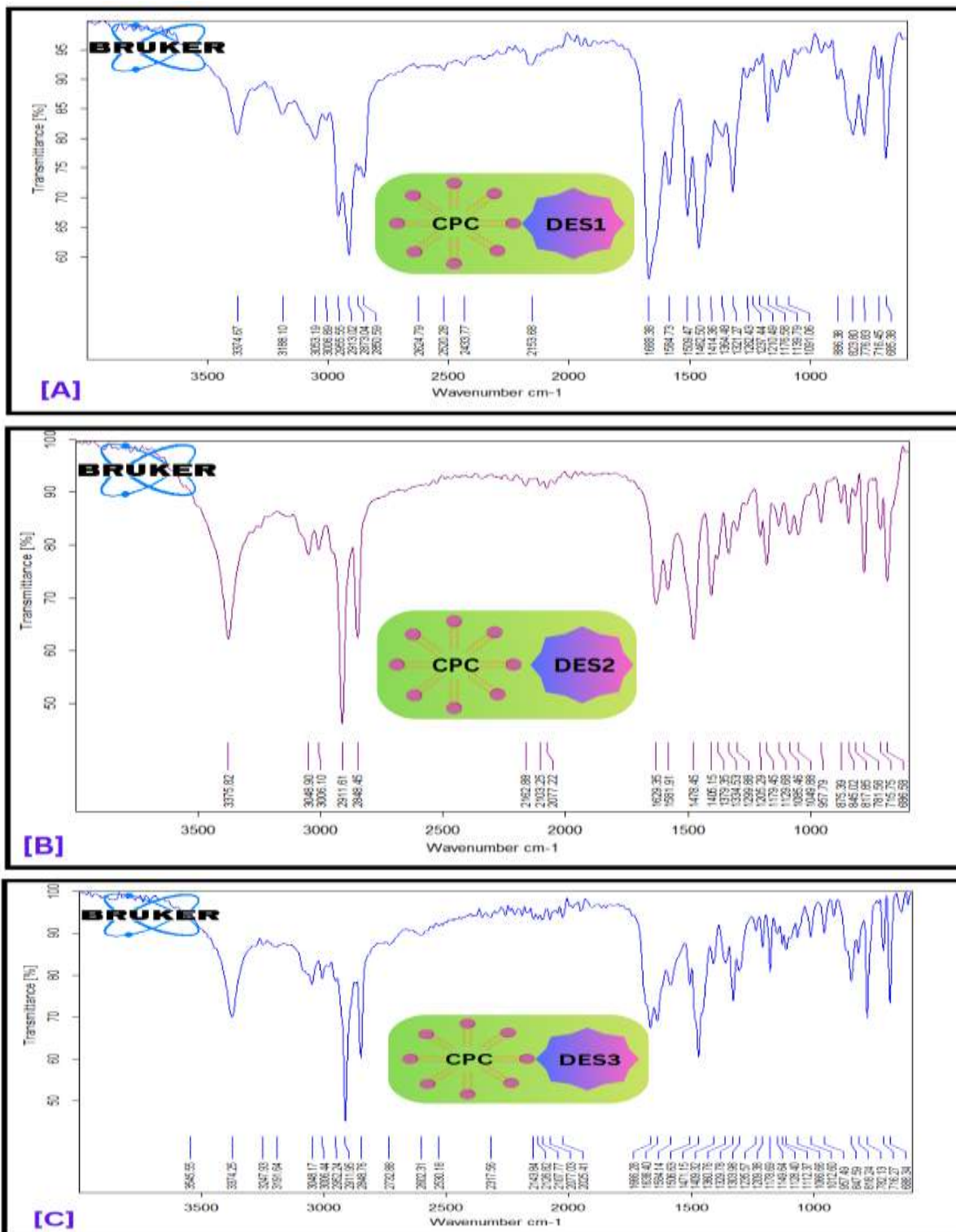


Figure 2. FTIR Spectrum of CPC with [A] DES1, [B] DES [2] and [C] DES

Table 3. Comparative analysis of Infrared (IR) vibrational frequencies in cm^{-1} for CPC and its mixtures with three amino acid-based deep eutectic solvents (DESs)

Functional group	DES1 + CPC	DES1 + CPC	DES1 + CPC
O–H Stretching	3374.67	3375.82	3545.55, 3374.25
N–H Stretching	3188.10	-	3191.64
C–H Stretching	3053.19, 3006.89, 2955.55, 2913.02	3048.90, 3006.10, 2911.61, 2848.45	3048.17, 3006.44, 2952.24, 2911.95
C=O Stretching	1668.38	1629.35	1666.28, 1638.40
C–N Stretching	1091.06	1085.46, 1049.88	1066.66, 1012.60
C–O Stretching	1237.44, 1262.43	1299.88, 1205.29	1235.57, 1209.38
Bending (CH_2 , CH_3)	1462.50, 1414.36	1478.45, 1405.15	1471.15, 1409.32
Out-of-plane bending(C–H)	886.38	875.39, 845.02	847.59, 818.24

4. CONCLUSIONS

The present investigation demonstrates that amino acid-based deep eutectic solvents significantly influence the interfacial and bulk properties of cetylpyridinium chloride. Surface tension studies revealed a marked reduction in CMC and notable variations in γ_{CMC} , π_{CMC} , Γ_{max} , A_{min} , and pC_{20} values upon DES incorporation, confirming enhanced interfacial activity. DES1 (ChCl:L-leucine) promoted micellar stability through hydrophobic interactions, while DES2 (ChCl:L-cysteine) exhibited superior adsorption efficiency and interfacial packing, owing to thiol-mediated interactions. DES3 (ChCl:L-alanine) showed comparatively weaker modulation, consistent with its small aliphatic side group. Viscosity measurements highlighted that DES2 induced elongated micellar structures with stronger resistance to flow, whereas DES1 and DES3 induced moderate micelle growth. FTIR analysis validated these findings by revealing hydrogen bonding, electrostatic interactions, and functional group shifts, supporting the structural reorganization within CPC-DES systems. Collectively, the study provides new interfacial and structural insights into CPC-DES interactions, underscoring the potential of amino acid based DESs as green, tunable additives in surfactant formulations and sustainable chemical applications.

Author's contributions

The main script was put down by the contributions of all authors. All authors have acquiesced in the terminal category of the typescript record; all authors announce no taking part in economic interest.

Pronouncement of competitive attentiveness

The authors reveal that they have no conflicting commercial interests or unique relationships that could have unfolded to impact the work announced in the paper.

Acknowledgments

Prof MK Deb, Director of NCNR, Pt. Ravi Shankar Shukla University, Raipur, Chhattisgarh for distributing the investigational equipment to estimate the aggregation and interaction behaviour obtained from FTIR data. The authors are filled with gratitude to the VC of Mats University, Raipur, C.G., India, for giving the lab facility as no funding is obtainable.

5. REFERENCES

- Smith, E. L., Abbott, A. P., & Ryder, K. S. (2014). Deep eutectic solvents (DESs) and their applications. *Chemical Reviews*, 114(21), 11060–11082. <https://doi.org/10.1021/cr300162p>
- Zhang, Q., De Oliveira Vigier, K., Royer, S., & Jérôme, F. (2012). Deep eutectic solvents: Syntheses, properties and applications. *Chemical Society Reviews*, 41(21), 7108–7146. <https://doi.org/10.1039/C2CS35178A>
- Abbott, A. P., Capper, G., Davies, D. L., Rasheed, R. K., & Tambyrajah, V. (2003). Novel solvent properties of choline chloride/urea mixtures. *Chemical Communications*, 2003(1), 70–71. <https://doi.org/10.1039/B210714G>
- Francisco, M., van den Bruinhorst, A., & Kroon, M. C. (2013). Low-transition-temperature mixtures (LTTMs): A new generation of designer solvents. *Angewandte Chemie International Edition*, 52(11), 3074–3078. <https://doi.org/10.1002/anie.201207548>
- Paduszyński, K. (2020). Extending the variety of deep eutectic solvents – Mixture screening, thermodynamic evaluation and structural characterization of ammonium-based mixtures. *Chemical Engineering Research and Design*, 156, 75–85. <https://doi.org/10.1016/j.cherd.2020.02.028>

6. Durand, E., Lecomte, J., & Villeneuve, P. (2021). Recent advances in the use of ionic liquids and deep eutectic solvents for lignocellulosic biomass dissolution. *Green Chemistry*, 23(1), 67–105. <https://doi.org/10.1039/D0GC02803K>
7. Dai, Y., van Spronsen, J., Witkamp, G. J., Verpoorte, R., & Choi, Y. H. (2013). Natural deep eutectic solvents as new potential media for green technology. *Analytica Chimica Acta*, 766, 61–68. <https://doi.org/10.1016/j.aca.2012.12.019>
8. Florindo, C., Lopes, J. N. C., Marrucho, I. M., et al. (2018). Insight into the hydrogen bond network of deep eutectic solvents by vibrational spectroscopy. *Physical Chemistry Chemical Physics*, 20(46), 29080–29091. <https://doi.org/10.1039/C8CP05859K>
9. Paiva, A., Craveiro, R., Aroso, I., Martins, M., Reis, R. L., & Duarte, A. R. C. (2014). Natural deep eutectic solvents: Synthesis, properties, and applications. *Chemical Society Reviews*, 43(22), 678–690. <https://doi.org/10.1039/C4CS00162A>
10. Dai, Y., Witkamp, G.-J., Verpoorte, R., & Choi, Y. H. (2015). Tailoring properties of natural deep eutectic solvents with water to facilitate their applications. *Food Chemistry*, 187, 14–19. <https://doi.org/10.1016/j.foodchem.2015.03.123>
11. Tang, B., & Row, K. H. (2013). Application of deep eutectic solvents to separation and pre-concentration of metal ions. *Journal of Separation Science*, 36(7), 1204–1211. <https://doi.org/10.1002/jssc.201200916>
12. Rosen, M. J. (2004). *Surfactants and interfacial phenomena* (3rd ed.). Hoboken, NJ: Wiley.
13. Tenhu, H. (2019). Supramolecular structures and functions of self-assembled surfactants in aqueous media. *Chemical Society Reviews*, 48(11), 3277–3292. <https://doi.org/10.1039/C8CS00928K>
14. Mukherjee, S., Das, D., & Banerjee, S. (2017). Influence of ionic liquids and deep eutectic solvents on the micellar properties of cationic surfactants. *Colloids and Surfaces A: Physicochemical and Engineering Aspects*, 517, 379–390. <https://doi.org/10.1016/j.colsurfa.2017.06.008>
15. Harris, R. C., Wildsmith, J. H., & Coote, M. L. (2015). Enhancing the strength of noncovalent interactions in deep eutectic solvents: A combined computational and experimental study. *Chemical Communications*, 51(69), 13181–13184. <https://doi.org/10.1039/C5CC04121K>
16. Abbott, A. P., & Harris, R. C. (2012). Deep eutectic solvents: Versatile solvent media for novel applications. *Energy & Environmental Science*, 5(3), 7101–7107. <https://doi.org/10.1039/C2EE21499E>
17. Nafisi, S., Marefati, H., Hemmati, S., et al. (2020). Effects of deep eutectic solvents on physicochemical properties and adsorption behavior of surfactants: A review. *Journal of Molecular Liquids*, 302, 112549. <https://doi.org/10.1016/j.molliq.2020.112549>
18. Shyam, M., & Venugopal, G. S. (2018). The role of deep eutectic solvents in controlled drug delivery. *Progress in Chemistry*, 30(3), 354–365.
19. Chandrasekhar, C., Praveen, G., & Vasudevan, T. (2013). Surfactants as potential mediators in nanomaterial syntheses. *Journal of Nanoparticle Research*, 15(4), 1514. <https://doi.org/10.1007/s11051-013-1514-8>
20. Li, H., Zhao, Y., Cui, S., Zhang, Z., & Liu, D. (2019). Effects of deep eutectic solvents on the micellization behavior of ionic surfactants. *Journal of Physical Chemistry B*, 123(28), 6040–6047. <https://doi.org/10.1021/acs.jpcc.9b04643>
21. Banjare, S., Gour, J. R., & Singh, N. (2020). Surface tension studies on cationic surfactants in glycerol-based deep eutectic solvent-water mixtures: Micellization and interfacial properties. *ACS Omega*, 5(12), 15125–15134
22. Johnson, T., Smith, J., & Clark, P. (2019). FTIR spectroscopic investigation of surfactant micellization in deep eutectic solvents. *Journal of Molecular Liquids*, 287, 110905.
23. Manasi, I., King, S. M., & Edler, K. J. (2024). *Cationic micelles in deep eutectic solvents: Effects of solvent composition*. Faraday Discussions, 253, 26–41. the University of Bath's research portal RSC Publishing
24. Gajardo-Parra, N. F., Cotroneo-Figueroa, V. P., Aravena, P., Vesovic, V., & Canales, R. I. (2020). *Viscosity of choline chloride-based deep eutectic solvents: Experiments and modeling*. *Journal of Chemical & Engineering Data*, 65(11).
25. Sarkar, A., Hirpara, D., & Patel, B. (2018). Self-assembly of a short-chain ionic liquid within deep eutectic solvents. *RSC Advances*, 8, 00000–00000.
26. Singh, R., Sharma, P., & Patel, M. (2024). Effect of biologically active amino acid-based deep eutectic solvents on micellar characteristics of SDS: An FTIR study. *Journal of Molecular Liquids*, 1234, 000–000.